Combustion of nanoaluminum and magnesium in fuel-rich propellants

Filippo Maggi*,[a] Francesco Zadra [a]

Abstract: Fuel-rich propellants are used in ducted rocket technology. The reduced content of oxidizer and the use of atmospheric air improve the gravimetric specific impulse far above the level of standard rocket motors, granting longer operating range. Peculiar requirements of ducted rockets favor either high or low pressure exponent propellants, depending on the pressurization strategy of the gas generator. The introduction of metal additives further improves the volumetric specific impulse and plays in favor of system compactness but combustion is difficult due to the intrinsic lack of oxidizer. Agglomeration of metal and low burning rates are observed. In this paper the combustion of a set of fuel-rich propellants is investigated. Reported data set comprise ideal performance, burning rate, incipient agglomeration, and metal content of the agglomerates.

Keywords: aluminized propellant, fuel-rich, agglomeration, metal content, ducted rockets

1 Introduction

Ducted rockets compare favorably with both standard rockets and turbojet engines for supersonic atmospheric missions. With respect to the former propulsion technology, they grant higher specific impulse leading to superior range. In comparison to the latter one, they extend air-breathing operations at higher Mach numbers [1,2]. Two combustion processes are involved. The primary one concerns a fuel-rich propellant, evenly termed gas-generating pyrolant, burning inside a gas-generator. The combustion products are injected in the secondary combustion chamber where they mix with the air coming from the supersonic inlet and complete the oxidation. The internal flow of the ram burner is subsonic [3]. With respect to typical liquid-fueled ramjets, ducted rockets feature a lower gravimetric specific impulse but are simpler to operate and have a higher propellant density.

Propellant compositions used in gas generators are characterized by low oxidizer content. A typical mass fraction of 25% to 50% is reported in the literature for compositions based on ammonium perchlorate (AP) [4], much lower than the properties of the energetic materials used in solid propellant rocket motors (AP content from 60% to 90%) [5]. Active binders, metal, and non-metal powders are also included as high-energy density fuels. Metals commonly adopted in this application are lithium, zirconium, aluminum, magnesium, boron, and titanium [6-9]. Combustion issues may arise. The decomposition of the inert polymer at the propellant surface can generate a skeletal-like carbonaceous layer when the oxidizing capability is reduced. On the other hand, metal additives can aggregate at the burning surface and generate large agglomerates requiring inadequate residence time in the ram burner to complete the combustion [10].

In general, the increment of metal reactivity fosters the reduction of agglomerate sizes. Metal powders capable of low ignition temperature (e.g. magnesium) release heat feedback in the proximity of the propellant-gas interface, leading to an increment of the burning rate and, thus, to a reduction of the metal residence time [11]. Similar effect was observed for nanoaluminum [12]. In addition, nanometric metallic powders can support the combustion of the coarser metal fraction, when used in bimodal mix. Beneficial effects have been observed for both powder suspensions and propellants [13-15]. The key role of metal reactivity has also been confirmed by experiments involving activated metal powders. These are classes of metal fuels that have been processed in a mechanical and/or chemical way, obtaining a reduction of the ignition temperature. Although these ingredients maintain a micrometric size, recent works have shown that the enhanced metal reactivity contributes to agglomeration reduction [16-18]. In this work, fuel-rich propellants based on AP oxidizer, hydroxyl-terminated polybutadiene (HTPB) binder and aluminum are considered. Addition of magnesium and nanoaluminum is investigated to ease the combustion of the main metal fuel. Earlier ignition is expected to generate stronger heat feedback towards the burning surface enhancing the quality of the metal combustion and of the inert binder, as well as incrementing the burning rate.

[a] *F. Maggi*
Dept. Aerospace Science and Tecnology
Politecnico di Milano
Via La Masa 34, 20156 Milano, Italy
E-mail: filippo.maggi@polimi.it

[a] *F. Zadra*
Dept. Aerospace Science and Tecnology
Politecnico di Milano
Via La Masa 34, 20156 Milano, Italy
E-mail: francesco.zadrai@mail.polimi.it

2 Materials

All compositions shared the same mass fraction of oxidizer, binder, and metallic fuel. These ones have been reported in Table 1. The oxidizer is a blend of coarse and fine AP powders. The coarse fraction (CAP) was a standard propulsion-grade oxidizer with nominal size of 200 μm. The fine fraction (FAP) was produced by grinding, using a Retsch PM 100 ball miller. Its mass-mean diameter was measured through laser granulometry analysis and resulted below 20 μm . A unique FAP production batch was used for the whole set of tests. The main metal fuel was a 30 μm propulsion-grade aluminum powder (μAl). A 20% fraction of Al was also replaced with magnesium powder having size 44 μm (μMg) in the composition AP50Al.Mg20, and with 100 nm uncoated nanoaluminum (nAl) in AP50Al.nAl20 propellant. The nAl was produced by means of EEW technique. The preparation was performed using a Labram Resodyn mixer under vacuum, according to standard internal procedure, reaching up to 100 g of acceleration.

Table 1. Propellant compositions in mass percent.

Label	CAP/FAP	HTPB	μAl	μMg / nAl
AP50Al(0)	50.0 / 0	14.0	36.0	0 / 0
AP50Al_base	44.0 / 6.0	14.0	36.0	0 / 0
AP50Al(12)	38.0 / 12.0	14.0	36.0	0 / 0
AP50Al.Mg20	44.0 / 6.0	14.0	28.8	7.2 / 0
AP50Al.nAl20	44.0 / 6.0	14.0	28.8	0 / 7.2

3 Ideal specific impulse

The ideal thermochemical performance of ducted rockets is influenced by both the flight conditions and the burning composition. A reference mission profile with an altitude of 15 km and a flight Mach number equal to 3.5 was selected, obtaining 748 K total temperature and 0.924 MPa total pressure at the intake. According to pressure recovery estimation from military specification MIL-E-5008B [19], the total pressure at the ram burner was assumed 0.685 MPa. Under the hypotheses of monophase and calorically perfect gas mixture, steady-state isentropic flow, and frozen chemical composition during the nozzle expansion, for an airbreathing device the optimal gravimetric and volumetric specific impulses can be obtained by Eq.1 and Eq.2, respectively.

$$I_{sp} = \frac{1}{g_0}\sqrt{\frac{2k}{k-1}\Re\frac{T_C}{\mathcal{M}}\left[1-\left(\frac{p_e}{p_C}\right)^{\frac{k-1}{k}}\right]}(1+\phi) - \frac{v_\infty \phi}{g_0} \qquad (1)$$

$$I_V = <\rho> \cdot I_{sp} \qquad (2)$$

Ram-burner combustion properties were computed under the assumptions of chemical equilibrium and stagnation flow. Performance data were evaluated for the air-to-propellant (A/P) mass ratio of 5.0, 7.5, 10.0. NASA CEA was used for chemical computation, using its internal database for ingredient properties [20,21], apart from HTPB ($C_{7.075}H_{10.65}O_{0.223}N_{0.063}$, $\Delta h_f^0 = -58\,\mathrm{kJ/mol}$ [22]). Air was considered at the stagnation temperature. The reduced active metal content of nanoaluminum was simulated by considering a 10% mass of aluminum oxide, which is a reasonable assumption according to the literature on nAl characterization [23]. It should be noted that compositions AP50Al(0), AP50Al_base, and AP50Al(12) from the thermochemical viewpoint are indistinguishable. Results are reported in Figure 1 and Figure 2.

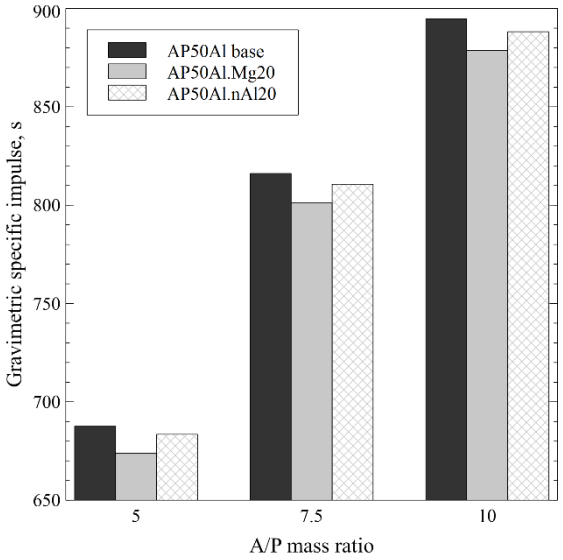

Figure 1. Gravimetric specific impulse for a reference mission (15 km altitude, Mach 3.5)

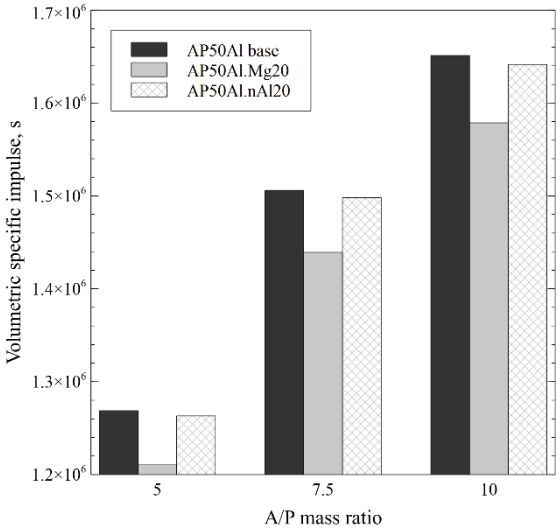

Figure 2. Volumetric specific impulse for a reference mission (15 km altitude, Mach 3.5)

As expected, the increment of the A/P ratio provides a higher gravimetric specific impulse due to

the incremented fraction of air used in the process. The partial replacement of micrometric aluminum causes minimal performance loss, limited to less than 2%. When the substitution is accomplished by Mg the decrement is about 1.5 to 2%. The loss introduced by the use of nAl is almost irrelevant, settling below 1%. In both cases the main reason consists of a slight reduction of the combustion chamber temperature due to different enthalpy released by the oxidation of the metal into its corresponding oxide.

The volumetric specific impulse for the propellant containing nAl is similar to the one of the baseline (about -0.5%). A decrement of about 4.5% is observed for the composition containing Mg. In this respect, part of the loss for the AP50Al.Mg20 propellant is attributed to the reduction of the TMD. The density of the AP50Al_base is $1845\ \mathrm{kg}/m^3$ while for the AP50Al.Mg20 is $1796\ \mathrm{kg}/m^3$, due to the different metallic additive (density of $1740\ \mathrm{kg}/m^3$ for Mg and $2700\ \mathrm{kg}/m^3$ for Al). On the other hand, the presence of aluminum oxide in the passivated layer of nAl increments the density of the metal particles from $2700\ kg/m^3$ to about $2720\ kg/m^3$. The resulting propellant AP50Al.nAl20 benefits from minimal increment of the TMD to $1848\ \mathrm{kg}/m^3$. The paper assumes the density of corundum aluminum oxide (alpha phase) which should be thoroughly verified. In fact, due to the limited thickness of the oxide layer, this crystalline structure may not form [24].

4 Experimental characterization

4.1 Burning rate

Propellant steady combustion properties have been tested in the SPLab vertical strand burner facility. The experimental rig is made by a stainless steel vessel of 2 dm^3 volume equipped with 4 optical accesses for propellant combustion video recording. A set of electrovalves controlled by an analog regulator maintains a constant pressure during the test with an accuracy of $\pm 2\%$ of the set point. Purging gas is nitrogen. Burning rate is measured through optical method by digitally recording a calibrated video of the propellant combustion and post-processing it through a proprietary software. The propellant strands were cut in samples of 4 mm x 4 mm x 30 mm, side-inhibited by a solution of low molecular weight polymer. Combustion tests have been performed at 2, 3, 4, and 5 MPa. Data were correlated through thestandard Vieille law $r_b = a\mathrm{p}_\mathrm{c}^\mathrm{n}$ to obtain the multiplicative factor a and the pressure exponent n. Experimental data are reported in Figure 3 while fitting results are reported in Table 2. Uncertainties have been computed using t-student distribution assuming 95% confidence. For a matter of reference, the same table reports the burning rate obtained by the respective Vieille's law at 5 MPa (r_{b5})

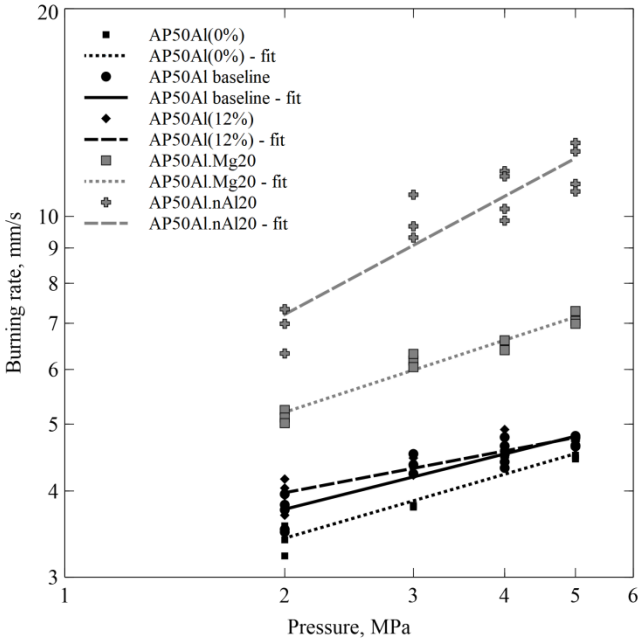

Figure 3. Burning rate data and respective fittings through Vieille's law

Table 2. Vieille's law of propellants with coefficient of determination. Pressure in MPa.

Label	Burning rate, mm/s	r_{b5}, mm/s	R^2
AP50Al(0%)	$2.76 \pm 0.09\ p^{0.308 \pm 0.027}$	4.50	0.934
AP50Al_base	$3.13 \pm 0.12\ p^{0.267 \pm 0.030}$	4.80	0.838
AP50Al(12%)	$3.46 \pm 0.12\ p^{0.201 \pm 0.029}$	4.79	0.800
AP50Al.Mg20	$4.09 \pm 0.13\ p^{0.347 \pm 0.025}$	7.20	0.954
AP50Al.nAl20	$4.86 \pm 0.44\ p^{0.569 \pm 0.070}$	12.2	0.846

4.2 Combustion residues

The collection of combustion residues has been performed in a 1.4 dm^3 stainless steel test chamber pressurized by nitrogen at 4 MPa. The pressure control and the sample preparation are similar to the ones already described for the strand-burner experiment. The arrangement makes the strand burn upside-down and release the condensed products inside a quenching pool placed below the combustion surface and filled with a chlorine-based hydrocarbon liquid. After the combustion, the system was kept under pressure for 10 minutes to let the deposition of light CCP. Then, residues were collected and processed for granulometry measurement through laser diffraction with Malvern Mastersizer 2000. Volume-mean diameters (D_{43}) are reported in Table 3. Uncertainty interval was estimated assuming a t-student distribution with 90% of confidence level.

A fraction of the CCPs was processed to quantify the aluminum mass content (C_{metal}) through

volumetric method. The technique consists in monitoring the moles of hydrogen evolved by hydrolysis in a water bath where sodium hydroxide (NaOH) is dissolved (5% m/m). The conversion between gas generation and original metal content is ruled by Eq. 3 [25]. Due to its reactivity and prompt ignition, magnesium was assumed to be completely oxidized and was not considered in this balance. Results of CCP metal content and volume-mean particle size are presented in Table 3 while their size distributions are reported in Figure 4 and Figure 5.

$$Al + 3H_2O \rightarrow Al(OH_3) + \frac{3}{2}H_2 + 459.1\ kJ \qquad (3)$$

Table 3. Volume-mean diameter and metal content mass fraction of CCP (4 MPa combustion pressure).

Label	D_{43}, µm	C_{metal}, %
AP50Al (0)	333.8 ± 9.9	N.Av.
AP50Al_base	397.7 ± 31.0	52.4
AP50Al (12)	446.6 ± 60.8	N.Av.
AP50Al.Mg20	241.6 ± 22.2	32.2
AP50Al.nAl20	325.3 ± 110.9	33.8

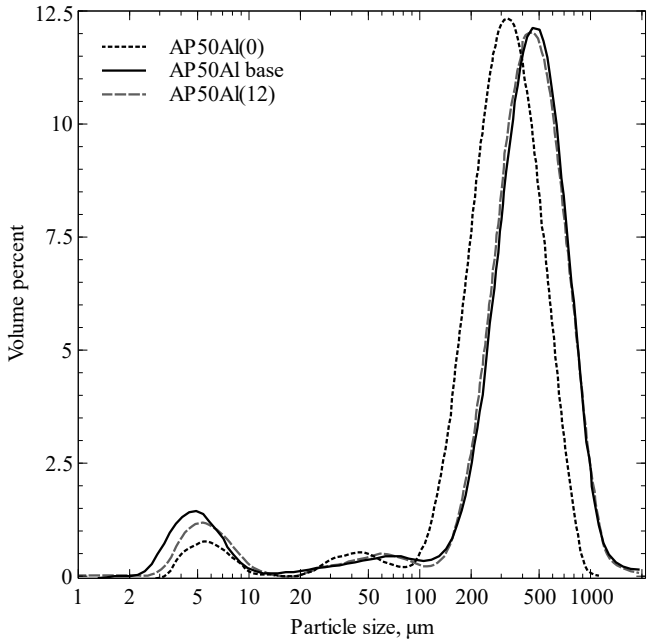

Figure 4. CCP size distribution: FAP variation (4 MPa combustion pressure)

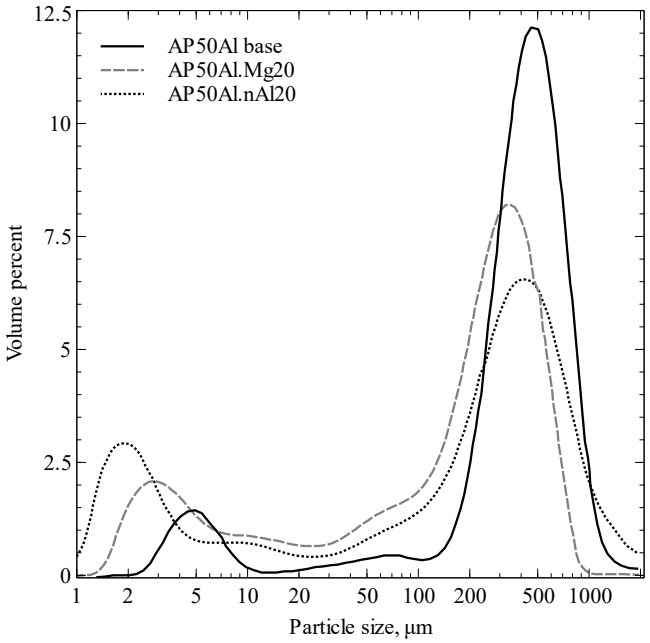

Figure 5. CCP size distribution: metal additives (4 MPa combustion pressure)

5 Discussion

The compositions based on standard µAl show limited reactivity. The burning rate is lower than 5 mm/s at 5 MPa and the pressure exponent is 0.308 or lower. In this respect the increment of the FAP fraction reduces progressively the pressure exponent. This trend is opposite than the behavior observed in propellants where the increment of fine AP fraction tends to promote an increment of the pressure exponent. It appears that, in the investigated pressure range, the solid phase decomposition is the dominant reaction and the gas phase chemistry does not have dominant roles. In this scenario, the slow burning rate is promoting the agglomeration of the micrometric aluminum. The distribution shows two distinct modes: the fine combustion products in the range between 2 and 10 µm and the coarse agglomerates between 100 and 1000 µm. In addition, a third family can be inferred between 20 and 100 µm. This group is clearly observed for the propellant AP50Al(0) and its dimensions coincide with the ones of the original metal particles suggesting that such particles underwent only limited modifications (minimal agglomeration or combustion). The addition of FAP moves slightly the agglomeration peak towards higher values, as demonstrated by the increment of the volume mean diameter of the collected CCP. Metal content measurements indicate that half of the collected particles are still composed by unreacted aluminum.

The partial replacement of micrometric aluminum with more reactive components changes some of the behaviors. The addition of magnesium leads to an incremented burning rate thanks to prompter ignition of this metal fraction. It is plausible that the micrometric aluminum takes advantage of the enthalpy released by the early magnesium ignition. The Vieille's law of AP50Al.Mg20 still reveals a low

exponent n equal to 0.347, although higher than the one obtained by the three initial compositions. Despite the distinctive modes are still present, the peak attributed to the agglomerates is reduced and shifted towards lower values, as also testified by the volume mean diameter. Similar considerations can be done for the propellant AP50Al.nAl20. In this last case, the Vieille's law demonstrates a completely different behavior. The pressure exponent increments to 0.569 and the burning rate at 5 MPa is almost three times higher than the baseline composition. The agglomeration trend is quite similar to the one provoked by magnesium, featuring a decrement of the main agglomeration peak and an increment of the fine CCP fraction. When compared with magnesium, the use of nanoaluminum shows different effect on combustion. Gas phase reactions turn to have stronger importance probably due to the additive incremented reactivity. The higher burning rate enables lower agglomeration. Also the CCP metal content decreases to 33.8% by mass, showing that part of the micrometric metal oxidizes along with the additive.

6 Conclusion

The tuning of fuel-rich aluminized compositions based on classical AP/HTPB combination has demonstrated that the increment of the FAP fraction does not represent a viable solution for the increment of the propellant combustion quality. Rather, the partial replacement of standard aluminum with more reactive materials has provided evident improvements of combustion quality and ballistic properties. Magnesium has shown the best results in terms of CCP size distribution, at the expense of lower gravimetric and volumetric specific impulse. Nano-aluminum demonstrates the strongest effect on the ballistic behavior, obtaining high pressure exponent and high burning rate propellants, though minimizing ideal performance losses. Specifically, in this last case, the performance increment enables the application of the composition to ducted rocket family, without using energetic binders or additives in the composition. Specific investigations should be reimplemented in the case of using active ingredients due to the altered heat balance at the propellant burning surface.

Symbols and Abbreviations

a	multiplicative factor (Vieille's law)
C_{metal}	active metal content by mass
D_{43}	volume-mean particle diameter
f	propellant-to-air mass ratio
g_0	standard acceleration gravity
I_{sp}	gravimetric specific impulse
Iv	volumetric specific impulse
k	specific heat ratio
n	exponential factor (Vieille's law)
M	molar mass
p_c	static pressure (combustion chamber)
p_e	static pressure (nozzle exit)
p_0	total pressure
R	universal gas constant
R^2	coefficient of determination
r_b	burning rate
r_{b5}	burning rate at 5 MPa
Tc	combustion chamber temperature
v_∞	flight velocity
Φ	air-to-propellant mass ratio
Δh_f^0	standard enthalpy of formation
<ρ>	propellant density
A/P	air-to-propellant mass ratio
AP	ammonium perchlorate
CCP	condensed combustion products
CPS	combination propulsion systems
DR	ducted rockets
EEW	electric explosion of wire
FAP	fine ammonium perchlorate
HTPB	hydroxyl-terminated polybutadiene
nAl	nanoaluminum
SRM	solid propellant rocket motor
TMD	theoretical maximum density

References

[1] E. Fleeman, *Sizing examples*, in: Tactical missile design, chapter 7, AIAA Educational Series, Reston, VA, USA, **2006**.

[2] W. H. Heiser and D. T. Pratt, Hypersonic Airbreathing Propulsion, AIAA Education Series, American Institute of Aeronautics and Astronautics, Washington, DC, USA, **1994**.

[3] R. S. Fry. A Century of Ramjet Propulsion Technology Evolution. *J Propul Power*, 20(1):27–58, 2004

[4] C. Perut. Propellants for Integral Rocket Ramjet Systems. In: A. Davenas, editor, *Solid Rocket Propulsion Technology*, chapter 12, Pergamon, Amsterdam, 1993.

[5] G. P. Sutton and O. Biblarz. *Rocket Propulsion Elements*. John Wiley & Sons, New York, NY, USA, 7th edition, 2001.

[6] S. Goroshin, A. J. Higgins, and M. Kamel. Powdered Metals as Fuel for Hypersonic Ramjets. AIAA Paper No. 2001-3919, 2001.

[7] B. K. Athawale, S. N. Asthana, and H. Singh. Metallised Fuel-Rich Propellants for Solid Rocket Ramjet: A Review. *Defence Sci J*, 44(4):269–278, 1994.

[8] L. T. DeLuca, F. Maggi, S. Dossi, V. Weiser, A. Franzin, V. Gettwert, and T. Heintz. High-Energy Metal Fuels for Rocket Propulsion: Characterization and Performance. *Chin J Expl Prop*, 6:1–14, 2013.

[9] B. Natan and A. Gany. Ignition and Combustion of Boron Particles in the Flowfield of a Solid Fuel Ramjet. *J Propul Power*, 7(1):37–43, 1991.

[10] F. Maggi, S. Colciago, C. Paravan, S. Dossi, and L. Galfetti. Exploratory Investigations on Metal-Based Fuels for Airbreathing Propulsion. Progress in Propulsion Physics 11 (2019) 699-712.

[11] A. Ishihara and M.Q. Brewster. Combustion Studies of Boron, Magnesium, and Aluminum Composite Propellants, *Combust Sci Technol*, 87(1-6):275-290, 1993.

[12] L. T. DeLuca, L. Galfetti, G. Colombo, F. Maggi, A. Bandera, V. A. Babuk and V. P. Sinditskii. Microstructure Effects in Aluminized Solid Rocket Propellants, *J Propul Power*, 26(4):724-732, 2010.

[13] Y. Huang and G. A. Risha and V. Yang and R. A. Yetter. Combustion of bimodal nano/micron-sized aluminum particle dust in air, *P Combust Inst*, 31:2001-2009, 2007.

[14] A. Dokhan, E.W. Price, J.M. Seitzman, and R.K. Sigman. The effects of bimodal aluminum with ultrafine aluminum on the burning rates of solid propellants.*P Combust Inst*, 29(2): 2939—2946, 2002.

[15] F. Maggi, S. Dossi, C. Paravan, S. Carlotti, and L. Galfetti. Role of Pressure and Aluminum Size in Solid Propellant CCP Generation, AIAA Paper No. 2017-5076, 2017.

[16] T.R. Sippel, S.F. Son, and L. J. Groven. Aluminum agglomeration reduction in a composite propellant using tailored Al/PTFE particles. *Combust Flame*, 161(1):311-321, 2014.

[17] H.M. Belal. Modifying burning rate and agglomeration size in aluminized composite solid propellants using mechanically activated metals. *Open Access Dissertations*, 975, Purdue University, 2016.

[18] S. Dossi, C. Paravan, F. Maggi, and L. Galfetti. Novel activated metal powders for improvement of hybrid fuels and green solid propellants. AIAA Paper No. 2016-4596, 2016.

[19] Anon., Military specification: engine, aircraft, turbojet and turbofan, general specification for, MIL-E-5007D*, Military Specifications and Standards*, DOD, USA, 1973.

[20] S. Gordon and B. J. McBride. *Computer Program for Calculation of Complex Chemical Equilibrium Compositions and Applications*. I, Analysis. NASA RP-1311, 1994.

[21] S. Gordon and B. J. McBride. *Computer Program for Calculation of Complex Chemical Equilibrium Compositions and Applications*. II, Users Manual and Program Description. NASA RP-1311, **1996**.

[22] N. Kubota. Energetics of propellants and explosives. In: *Propellants and Explosives*, second edition, chapter 4, table 4.3, page 80, Wiley-VCH, Weinheim, Germany, **2007**.

[23] C. Paravan, F. Maggi, S. Dossi, G. Marra, G. Colombo L. Galfetti, Pre-burning Characterization of Nanosized Aluminum in Condensed Energetic Systems, in: *Energetic Nanomaterials* (Eds.: V. E. Zarko, A. A. Gromov) Elsevier, Amsterdam, NL, **2016**, pp. 341-368.

[24] E. W. Dreizin, Metal-based reactive nanomaterials, *Prog. Ener. Combust.* **2009**, 35, 141-167.

[25] A. P. Astankova, A. Yu. Godymchuk, A. A. Gromov, A. P. Il'in, The kinetics of self-heating in the reaction between aluminum nanopowder and liquid water, *Russ. J. Phys. Ch.* **2008**, 82, 1913-1920.